RESEARCH ARTICLE

Bone Sialoprotein Immobilized in Collagen Type I Enhances Bone Regeneration In vitro and In vivo

Anja Kriegel[1], Christian Schlosser[1], Tanja Habeck[1], Christoph Dahmen[1], Hermann Götz[2], Franziska Clauder[3], Franz Paul Armbruster[3], Andreas Baranowski[1], Philipp Drees[1], Pol Maria Rommens[1], Ulrike Ritz[1]*

[1]Department of Orthopedics and Traumatology, University Medical Center of the Johannes Gutenberg-University, Mainz, Germany
[2]Cell Biology Unit, PKZI, University Medical Center of the Johannes Gutenberg-University, Mainz, Germany
[3]Immundiagnostik AG, Bensheim, Germany

Abstract: The use of bioactive molecules is a promising approach to enhance the bone healing properties of biomaterials. The aim of this study was to define the role of bone sialoprotein (BSP) immobilized in collagen type I in various settings. In vitro studies with human primary osteoblasts in mono- or in co-culture with endothelial cells demonstrated a slightly increased gene expression of osteogenic markers as well as an increased proliferation rate in osteoblasts after application of BSP immobilized in collagen type I. Two critical size bone defect models were used to analyze bone regeneration. BSP incorporated in collagen type I increased bone regeneration only marginally at one concentration in a calvarial defect model. To induce the mechanical stability, three-dimensional printing was used to produce a stable porous cylinder of polylactide. The cylinder was filled with collagen type I and immobilized BSP and implanted into a femoral defect of critical size in rats. This hybrid material was able to significantly induce bone regeneration. Our study clearly shows the osteogenic effect of BSP when combined with collagen type I as carrier and thereby offers various approaches and options for its use as bioactive molecule in bone substitute materials.

Keywords: Osteogenesis; 3D printing; Polylactide; In vivo critical size defects; Bone regeneration

***Correspondence to:** Ulrike Ritz, Department of Orthopedics and Traumatology, University Medical Center of the Johannes Gutenberg-University, Mainz, Germany; ritz@uni-mainz.de

Received: April 4, 2022; **Accepted:** May 23, 2022; **Published Online:** July 12, 2022

(This article belongs to the *Special Issue: Integrated Biofabrication Technologies for Constructing Functional Tissue*)

Citation: Kriegel A, Schlosser C, Habeck T, *et al*., 2022, Bone Sialoprotein Immobilized in Collagen Type I Enhances Bone Regeneration In vitro and In vivo. *Int J Bioprint,* 8(3):591. http://doi.org/10.18063/ijb.v8i3.591

1. Introduction

In orthopedics and trauma surgery, implants made of various (bio-)materials are frequently applied as bone substitutes. Main challenges in this area are to find an alternative for the gold standard of autogenous bone grafting and to improve implant osseointegration.

One approach to improve osseointegration of existing implants or biomaterials is their modification with extracellular matrix (ECM) components. The organic phase of the ECM contains collagen type I, proteoglycans, and non-collagenous proteins, such as bone sialoprotein (BSP), osteocalcin, osteonectin, thrombospondin, and osteopontin[1]. BSP belongs to the small integrin-binding ligand N-linked glycoprotein family and is expressed by various cells, among others by osteoblasts, osteocytes, and osteoclasts[2]. Besides the RGD-motif, the BSP structure contains tyrosine-rich regions, which affect cell adhesion, a collagen-binding sequence, and glutamine acid regions[3]. BSP binds $\alpha_v\beta_3$ and $\alpha_v\beta_5$ integrins, thereby mediating cell signaling and differentiation[4]. Lack of BSP (e.g., BSP-knockout) impairs bone formation processes, resulting in shorter as well as hypomineralized bones[5-8]. In BSP-knockout mice, bone formation

as well as resorption are impaired[9]. Moreover, BSP plays a major role in endochondral bone development and mineralization[10]. These results show that BSP is engaged in bone formation making it an interesting candidate for implant and biomaterial functionalization for bone regeneration, which could explain why it was used for functionalization of implant materials in this study. However, further exploration on which material is the best to be used as a scaffold and carrier material for this protein is required. Various materials have been modified with BSP and different effects related to gene expression, cell proliferation, or cell differentiation in vitro were observed[11-13]. For example, BSP-coated calcium phosphate cements (CPCs) demonstrated no superiority over pristine CPC concerning bone growth in two different in vivo models[12,14,15].

One promising candidate to be employed in tissue engineering and as scaffold is collagen type I, which has been widely studied during the last years[16]. Like BSP, it is a component of the ECM[17] and demonstrates various positive properties, besides being inexpensive, biocompatible, and non-allergic and the fact that it can be degraded by collagenases, thereby releasing non-toxic components. Moreover, bioactive molecules can be immobilized in collagen type I[18]. Literature shows that collagen type I and BSP interact with each other[18,19] and some studies combined BSP with collagen and observed a positive effect on osteoblast differentiation and bone repair[20,21]. Consequently, the hypothesis that collagen might be the optimal carrier for BSP has been proposed first by Kruger *et al*.[22] and was further supported by the fact that a complex of BSP and collagen is involved in bone mineralization[23]. However, one problem concerning collagen type I is its low stability especially when collagen is combined with osteogenic biomolecules, which is supposed to be used in bone tissue engineering.

One possible solution is to combine collagen with hard materials, for example, with polymer filaments such as polylactic acid (PLA), polycaprolactone, or polyether ether ketone. Besides their positive properties concerning biocompatibility, these materials can be used for three-dimensional (3D) printing to fabricate mechanically stable structures needed for bone regeneration and implantation. One of the most widely used polymers for 3D printing is PLA. PLA demonstrates the necessary properties such as biocompatibility and biodegradability. It is non-toxic and allows cell adhesion without being bioactive itself[24]. Its melting temperature of Ca. 175°C makes it an ideal candidate for 3D printing. However, due to the high temperature, bioactive molecules cannot be mixed with the material before printing, but the material can be combined with soft polymers[25], in which bioactive molecules can be immobilized.

We and others combined PLA and collagen to take advantage of the different properties of these materials: The mechanical stability of polylactide, although lower than bone, is still high enough to be used as bone substitute[26], and the soft material collagen, which can be modified with various bioactive molecules[18]. We and others printed PLA together with collagen to induce tissue regeneration in different bone defects[26,27]. It has been demonstrated that printed PLA scaffolds combined with collagen stimulated osteogenic properties such as adhesion and proliferation of osteogenic cells as well as alkaline phosphatase activity and osteogenesis-related gene expression in different cell types[28,29]. The combination of BSP, collagen type I, and polylactide seems to be a promising candidate to develop a new bone substitute material.

Taking into account these preliminary results, the aim of this study was to further analyze the effects of BSP immobilized in collagen type I. First, in vitro analyses with primary human osteoblasts (hOBs) and endothelial cells were performed. This 3D coculture model was chosen to imitate the physiological surroundings. Afterward, two rat models of critical size defects were used: A calvarial defect model and a femora defect model in combination with 3D-printed polylactide to provide the necessary mechanical stability for materials used in bone tissue regeneration. The goal of this study was to establish a cell-free bone substituting biomaterial consisting of collagen type I with incorporated BSP that can be easily produced.

2. Materials and methods

2.1. Cell culture

Primary hOBs were isolated according to a previously described protocol[30]. Human bone specimens were obtained during hip or knee joint replacement surgeries. The use of residual materials was approved by the ethics committee of the Landesärztekammer Rheinland-Pfalz in agreement with the university medical center and in accordance with the principles expressed in the Declaration of Helsinki and the ICH Guidelines for GCP. All patients provided written consent.

Human umbilical vein endothelial cells [HUVECs], PromoCell, Heidelberg, Germany, were cultured as recommended by the supplier.

2.2. Preparation of collagen gels (modified based on the protocol from Wenger *et al*.[31])

Three-dimensional collagen gels with a concentration of 2 mg/mL collagen type I (rat tail, BD Biosciences, Heidelberg, Germany) were used and prepared with 65% collagen solution (5 mg/mL), 10% medium 199 (10×), 6% $NaHCO_3$ (7.5%), 2.5 % NaOH (1 N), and 16.5% Aquadest (all from Sigma-Aldrich, Steinheim,

Germany). BSP (Immundiagnostik, Bensheim, Germany) was added directly into the gels (1 μg/mL and 5 μg/mL BSP), and therefore, the amount of Aqua was adjusted. Cell concentrations used were 5×10^5/mL either in hOB monoculture or 2.5×10^5/mL of each cell type for coculture of HUVEC and hOB. A 1 mL of collagen gel with or without BSP and cells was pipetted in 24 wells for following experiments. Gelification took place by a change of temperature by incubation at 37°C in an incubator for 20 min.

Release of BSP was measured after immobilization of 100 ng or 500 ng BSP in collagen gels employing a BSP-ELISA (Immundiagnostik, Bensheim, Germany), according to the manufacturer's instructions.

2.3. Viability assay

Cell viability of hOB mono- as well as co-cultures with HUVECs in prepared collagen gels (0 μg/mL, 1 μg/mL, and 5 μg/mL BSP) was analyzed on days 1, 2, 4, and 7 with the alamarBlue® assay (Life Technologies, Karlsruhe, Germany), according to the manufacturer's instruction. Collagen gels without cells and supplements served as an internal control.

2.4. RNA isolation/reverse transcription/ quantitative real-Time PCR

According to the viability assay, collagen gels without and with BSP supplementation (1 μg/mL and 5 μg/mL) were prepared. Cell number was adapted to 1×10^6 cells/well (coculture: 5×10^5 cells/well for each cell type). After 1, 4, and 7 days, the gels were digested using a 1 mg/mL collagenase I/dispase solution. The cell suspensions were centrifuged at 1400 rpm for 5 min and the cell pellet was stored at −80°C until RNA isolation. Isolation of RNA was conducted with the PeqGold Total RNA Micro Kit, according to manufacturer's instruction. Total RNA (1 μg) was reverse transcribed into cDNA using dNTPs (4you4 dNTPs Mix [10 mM], BIORON GmbH, Ludwigshafen), Random Primers (Promega, Madison, WI, USA), and MuLV RT (M-MuLV Reverse Transcriptase, M0253S New England Biolabs, Ipswich, MA, USA), according to the manufacturer's instructions. For gene expression analyses, cDNA template underwent PCR amplification (40 cycles) using the SYBR Green (PowerUp™ SYBR® Green Master Mix, Applied Biosystems, Foster City, CA, USA) and sequence specific primers (Primer sequences listed in **Table S1**). *GAPDH* was used to normalize gene expression. Results were calculated using the well-established $2^{-\Delta\Delta Ct}$ method[32].

2.5. *In vivo* models

This study was approved by the local regional welfare committee (Landesuntersuchungsamt Rheinland-Pfalz AZ 23 177-07/G 17-1-055 – calvarial model and AZ 23177-07/G17-1-032 for the femur defect model). All animal experiments complied with the Animal Research: Reporting of In vivo Experiments guidelines and were carried out in accordance with the EU Directive 2010/63/EU for animal experiments.

Two animals were housed per cage with a 12 h dark-light rhythm. Anesthesia was initiated with isoflurane-oxygen per inhalation. Rats were anesthetized with an intraperitoneal injection of midazolam (0.15 mg/kg), medetomidine (2 mg/kg), and fentanyl (0.005 mg/kg). As a pain prophylaxis, drinking water was supplied with tramadol (1 mg/mL) from 3 days before until 7 days after surgery.

2.5.1. Calvarial model

Forty-eight 10-week-old Wistar rats (Janvier, France) were acclimatized for 3 days before they were subdivided into four groups according to **Table S2**. Anesthesia was performed as described above and the parietal bone was uncovered by anatomical tweezers. Two bone defects were carefully set with a hollow drill (ø 5 mm) with parallel saline washing. The bone disks were removed, and the condition of the dura mater was checked. The rats were assigned into groups as follows: No treatment (Group 1) or differently loaded collagen gels were implanted (Group 2: Collagen gel alone, Group 3: Collagen gel + 0.5 μg BSP, and Group 4: Collagen gel + 5 μg BSP, **Table S2**).

Collagen gels were prepared as described in Section 2.2. A 500 μL of gels were used for the experiments and supplemented with 0, 0.5, or 5 μg BSP. The prepared collagen gels were implanted in the borehole defects and the wound was sutured with a simple interrupted stitch and disinfected. After 3 and 8 weeks, rats were killed by CO_2 intoxication and bleeding. The decapitated head was fixed with 4.5% formaldehyde solution for a minimum of 3 days.

Bone formation was evaluated using a high-resolution microcomputed tomography (μCT) scanner (CT 40, SCANCO Medical AG, Brüttisellen, Switzerland). μCT analyses were performed with 70 kV and 114 μAmp, the voxel size was set to 30 μm. μCT data were analyzed with ImageJ[33] and the BoneJ Plugin[34] was used for calculating the bone volume/total volume (BV/TV) fraction.

2.5.2. Femur defect model

A hollow cylinder with macropores of PLA filament (Ultimaker silver metallic PLA, iGo3D, Hannover, Germany) with a diameter of 4 mm and a height of 7 mm was printed with the Ultimaker 2+ as described before[26]. The collagen solution was prepared separately as described in 2.2. In total, 100 μL of this

solution was supplemented with 0.5 µg and 5 µg BSP or 2 µg BMP-7, respectively, and pipetted manually into the 3D-printed PLA cylinder and polymerized at room temperature for 30 min. **Figure 1A** shows the printed cylinder filled with collagen corresponding to an excised piece of rat femur. For release kinetics, the cylinder loaded with BSP was placed in 500 µL PBS. Complete supernatants were collected and replaced by fresh PBS after 1, 2, 4, 24, 48, and 72 h and the BSP content was measured using a specific ELISA (Immundiagnostik, Bensheim, Germany) as described by the manufacturer. The release was calculated as percentage in relation to the loaded amount of BSP, which was set to 100%.

Fifty-two 10-week-old Wistar rats (Janvier, France) were acclimatized for 3 days before they were subdivided into four groups according to **Table S3** (as negative controls an empty defect [$n = 6$] and PLA alone [$n = 6$], as test groups PLA + collagen alone [$n = 10$] or loaded with two different BSP concentrations and as positive control loaded with BMP-7 [each $n = 10$]). Anesthesia was performed as described above. To create the desired femoral osteotomy of 6 mm in length, we used the rat fix system (RISystem, Davos, Switzerland) as described before[26]. The PLA cylinder was set in the defect without further fixation (**Figure 1B**, arrow). The wound was closed with resorbable Vicryl sutures 4-0 (Ethilon, Ethicon, Norderstedt, Germany). X-rays were performed directly after surgery (**Figure 1C**, the PLA cylinder is not visible in the X-ray, but its position is marked with the arrow) and after 2, 4, and 8 weeks. The rats were sacrificed 4 ($n = 26$) and 8 weeks ($n = 26$) after surgery by exposure to CO_2. Femora were placed in 4.5% paraformaldehyde solution for µCT and histological analyses.

Bone formation was evaluated using a high-resolution microcomputed tomography (µCT) scanner (CT 40, SCANCO Medical AG, Brüttisellen, Switzerland) and analyzed as described before[26]. For generation of 3D graphics, the software Osirix (aycan, Würzburg, Germany) was used.

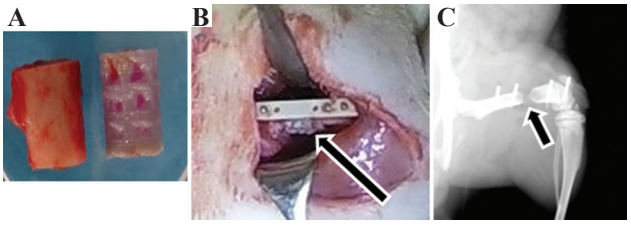

Figure 1. (A) 3D-printed PLA cylinder filled with collagen type I corresponding to an excised piece of rat femur. (B) PLA cylinder press-fit set in the created defect and (C) X-ray directly after surgery. The position of the not visible PLA cylinder (appearing as a hole and marked with an arrow).

2.6. Histology

2.6.1. Calvaria model

After radiologic analysis, the skulls were decalcified using a 10% EDTA solution for at least 8 weeks, with the solution exchanged every 2nd day during the first 2 weeks and then weekly. The skulls were dehydrated by the Sakura VIP E150 Tissue Processor (Sakura Finetek GmbH, Rüsselsheim, Germany) and then embedded in paraffin wax. The resulting blocks were cut in 5 µm slices, deparaffinized, and then stained with hematoxylin and eosin (HE).

2.6.2. Femora model

Femora were sent to LLS Rowiak (Hannover, Germany) for laser-based dissection and histology (HE and Masson-Goldner trichrome staining). Quantification of bone area was performed with ImageJ and the plugin color deconvolution 2.

2.7. Masson-Goldner Trichrome Staining

Nuclei were stained for 5 min with hematoxylin according to Weigert, washed with 1% acetic acid followed by Ponceau-S staining (Sigma-Aldrich, Darmstadt, Germany) for 10 min. After another washing step with acetic acid (1%), samples were placed in acid orange G solution (Carl Roth, Karlsruhe, Germany) for 10 min. After rinsing in 1% acetic acid, samples were stained with light green (Merck Chemicals GmbH, Darmstadt, Germany) for 10 min, then rinsed again in 1% acetic acid for 30 s.

2.8. Elastica van Gieson staining

Nuclei were stained for 5 min with hematoxylin according to Weigert then rinsed with distilled water for 10 min. After staining with resorcinol-fuchsine solution (Waldeck GmbH and Co. KG, Münster, Germany), samples were again rinsed with distilled water for 10 min. Then, samples were incubated with van Gieson solution (fuchsin-picric acid; Waldeck GmbH & Co. KG, Münster, Germany) for 5 min, dehydrated in alcohols, cleared, and mounted.

2.9. Statistical analyses

Statistical analyses were performed using the SPSS software (IBM, Version 23) or GraphPad Prism software. The results are presented as medians and quartiles or as means ± standard deviation. Measurements were carried out in triplicates, except for ELISA measurements (duplicate). Cell-based experiments were independently repeated 3 times with osteoblasts from different donors. Normally distributed data were analyzed by one-way ANOVA. Depending on Levene's test for equality of variances, pairwise comparisons were conducted either

by a Tukey-HSD or Games-Howell *post hoc* test. In contrast, non-normally distributed data were evaluated with the Kruskal–Wallis test. For pairwise comparisons, the Mann–Whitney U-test was used. $P < 0.05$ was considered statistically significant ($*P < 0.05$, $**P < 0.01$, and $***P < 0.001$). Due to multiple testing, the *P*-values were adjusted through Bonferroni-Holm method.

3. Results and discussion

3.1. BSP immobilized in collagen type I enhances proliferation of hOB in mono and in coculture

The first step to characterize the effect of BSP immobilized in collagen type I were in vitro assays. hOBs were seeded in collagen type I gels with and without BSP (**Figure S1**) and proliferation was analyzed using the alamarBlue assay (**Figure S2A**). Next proliferation in a coculture model with endothelial cells was analyzed as it has been demonstrated that this system is effective in regulating cell proliferation and osteoblastic differentiation (**Figure S2B**). **Figure S2** demonstrates that BSP applied in low concentrations enhanced proliferation of primary hOBs in mono- and in co-culture with endothelial cells. The most significant effect was observed after 4 days.

Regarding morphology of hOBs, no differences were observed whether they were seeded in mono- or in co-culture with HUVECs (**Figure S1**). One varying aspect in co-culture is the ratio of hOB and HUVECs. In our experiments, we used a ratio of 1:1; ratios ranging up to 1:10 have been described depending on the endothelial cell type used[35,36]. However, in our setting, the ratio of 1:1 has shown to be best[30].

Comparing the effects of BSP coated materials on different cells, varying effects were observed. Moreover, the materials used as well as the conditions employed varied making comparisons difficult. When human primary osteoblasts were seeded on titanium implants, a rather suppressive effect of BSP on proliferation was detected[11]. Regarding cell proliferation on calcium phosphate scaffolds, a low concentration of BSP could enhance proliferation of human primary osteoblasts to a small extent 3 days after seeding[12]. Other studies demonstrated that BSP coating showed no positive influence on cell proliferation[37]. However, this effect could also be an indication for increased osteogenicity as several studies have demonstrated that an increase in osteogenic activity is correlated to a decrease in cell proliferation[6,38,39].

An increase in proliferation can also be observed when cells are cultured in coculture. As described by several authors, endothelial cells and osteoblasts influence proliferation and differentiation of each other due to growth factor release[40]. Another remarkable point is the BSP concentration applied. In our experiments, the lower BSP concentration demonstrated a better effect on proliferation than the 5 times higher concentration speaking for a concentration dependency, also demonstrated in another study with BSP on titanium[11]. It might be that BSP in higher concentration effects other cells engaged in bone remodeling, for example, osteoclasts[8], however, this has to be addressed in follow-up experiments using other cells as well as wider concentrations ranges.

In summary, BSP was able to induce proliferation of hOB in mono- as well as in co-culture speaking for a positive effect, when BSP is applied in combination with collagen type I.

3.2. Effect of BSP encapsulation in collagen gels on gene expression in hOB monoculture

To further understand the effect of BSP encapsulated in collagen type I, gene expression analyses were performed. The ALP expression of hOBs was significantly downregulated in collagen gels containing 5 μg/mL BSP after 1 day as well as in gels with 1 μg/mL BSP after 4 days. However, expression increased after 7 days with the lower BSP concentration of 1 μg/mL (**Figure 2A**). Gene expression analyses of hOB monocultures revealed a decreased expression of OPN after BSP addition (**Figure 2B**). After 4 days, two key factors of osteoblastic differentiation were upregulated (SP7 in all BSP groups and RUNX2 in high concentrated BSP gels (**Figure 2C and D**).

3.3. Effect of BSP encapsulation in collagen gels on gene expression in hOB and HUVEC coculture

To imitate the physiological surroundings, cocultures of hOB and HUVEC were analyzed to detect intercellular influences. In cocultures, the trend in gene expression of osteogenic markers was similar to those of hOB monocultures. Significant changes occurred merely after 4 days of culture. OPN (1 and 5 μg/mL BSP; **Figure 2F**) as well as RUNX2 (5 μg/mL BSP, **Figure 2G**) expression increased. In coculture examinations, the SP7 expression was not affected by BSP supplementation (**Figure 2H**) in contrast to a significant upregulation by both BSP concentrations in hOB monocultures.

Enhancement of the transcription factors RUNX2 and SP7 gene expression caused by BSP employing various coating or expression methods as well as different materials (titanium, calcium-phosphate-cements, cell culture materials, etc.) has already been demonstrated in various studies[4,11,12,41]. The observation of higher RUNX2 and SP7 levels on day 4 compared with those on day 7 is consistent with the findings of Gordon *et al*. who showed that supplementation of 2 μg/mL BSP to primary rat calvaria osteoblasts significantly increased SP7 and

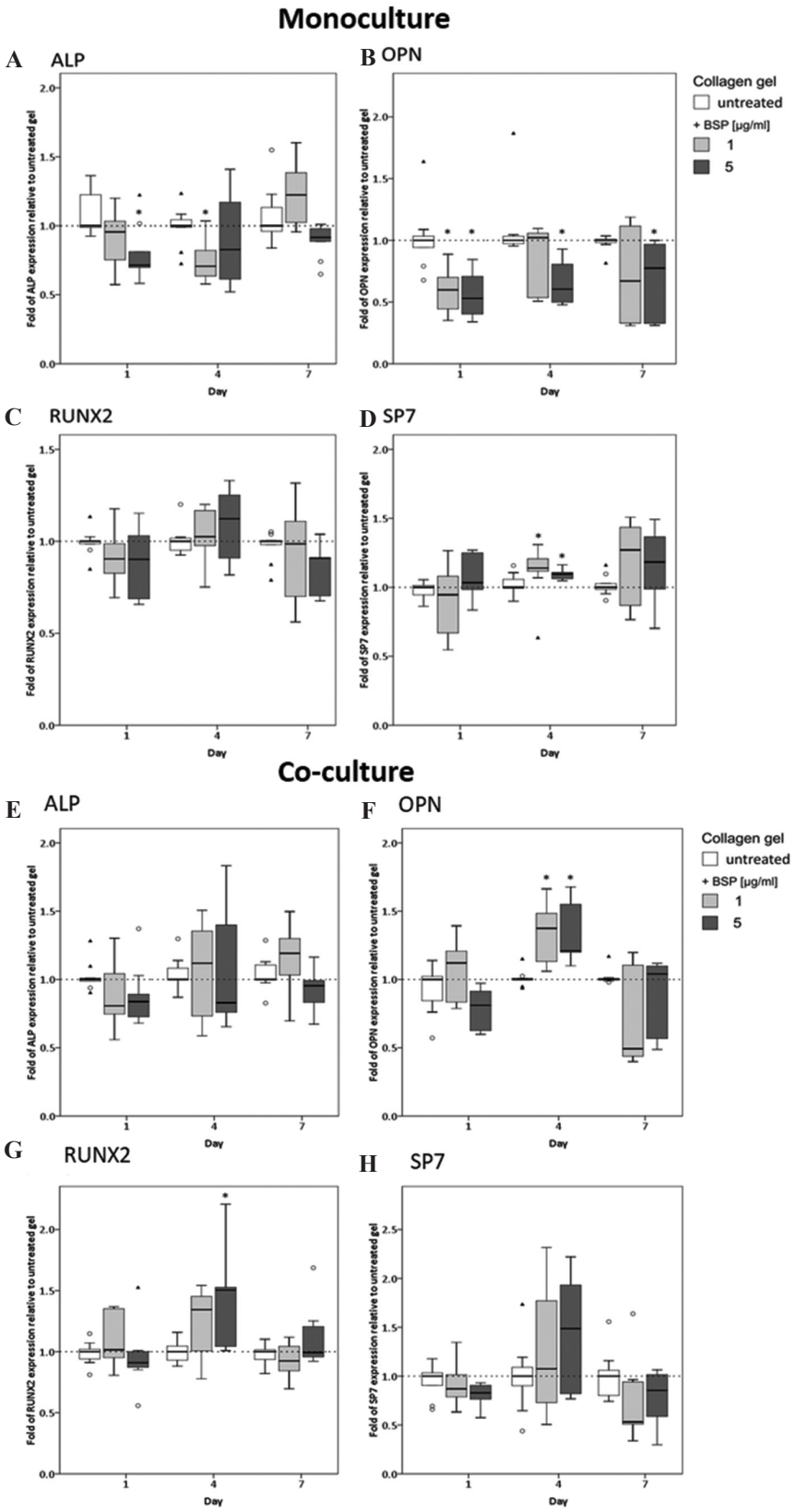

Figure 2. Relative alkaline phosphatase, osteopontin, Runx2, and SP7 gene expression of hOBs in mono- (A-D) and co-culture with endothelial cells (E-H) seeded in different modified collagen gels were compared with untreated collagen gels (gene expression = 1). Results are expressed as median and quartiles ($n = 9$). Mann–Whitney U-tests revealed significant differences (*$P < 0.05$, circles present outliners).

RUNX2 gene expression after 3 and 5 days compared with those in untreated osteoblast cultures[4]. In addition, enhanced relative RUNX2 and SP7 mRNA expression was detected in human MSCs seeded onto titanium surfaces functionalized with BSP by Im *et al*.[11,41]. In monoculture, expression of OPN was decreased after addition of BSP. As these two molecules have been described as molecules that can overtake the function of each other and influence their reciprocal expression, this is not surprising[6].

Moreover, Gordon *et al*. as well as Im *et al*. boosted cell differentiation by adding supplements such as ascorbic acid, β-glycerol phosphate, and dexamethasone[4,41]. Effects, depending on different concentrations, were observed for physisorbed BSP on titanium only on day 4[11]. Coating with a 280 μg/mL BSP solution displayed higher gene expression rates of ALP, Col1, SPARC, RUNX2, and SP7 compared with those of the lower concentration of 50 μg BSP/mL. However, no tendencies were observed after 7 days. Modification through covalent coupling showed on day 4 a tendency for increased expression by the lower BSP concentration (particularly for ALP, RUNX2, and SP7 mRNA expression). This is in contrast with the findings on day 7, which indicate a higher effect by coating with 280 μg/mL BSP (RUNX2, SP7, and SPARC). On CPC scaffolds, BSP concentrations of 50 μg/mL decreased gene expression of ALP and SPARC, whereas 200 μg/mL did not change marker expression[12]. Coating of BSP on ceramic and synthetic polymer materials with concentrations of 1 μg/mL and 10 μg/mL BSP showed no influence on hMSC differentiation in vitro as well as in vivo[42].

Taking into account, the described effects in literature and comparing them with our results, one can conclude that rather low concentrations of BSP influence osteogenic marker gene expression. However, it seems that the effect varies depending on the analyzed cell type and depending on the material employed as carrier material. We hypothesized that the best impact is obtained when BSP is immobilized in collagen, a component of the ECM. This hypothesis is supported by the fact that BSP contains a highly conserved collagen-binding domain, which explains why a binding and thereby immobilization of the molecule in a collagen type I gel is possible[19]. The characterization of the interaction between type I collagen and BSP has been described before. Very early works from Fujisawa *et al*. showed that BSP was absorbed to the collagen fibrils and preferentially bound to the α 2 chain[43]. Tye *et al*. showed that the binding of BSP to collagen type I is hydrophobic[19]and Baht *et al*. demonstrated higher affinities for helical domains[44], which are also present in the collagen used in this study. They also demonstrated a concentration dependent binding curve, with a saturation at a concentration of 200 nM approximately corresponding to the used concentration of 5 μg in this study.

3.4. Calvaria defect model

To test the effect of immobilized BSP in collagen type I in vivo, we performed an in vivo model to analyze fracture healing in a critical size defect model in the calvaria of rats. Various small animal models exist to characterize bone regeneration. We chose rats as model as they are the standard model to test new biomaterials for studies on bone regeneration and physiology as their bone biology is similar to humans. For the first study, a critical size defect in the calvaria was employed, which is a standard model for testing new materials. We chose the standard size for critical size defects in calvarial rat models of 5 mm[45]. BMP-7 was used as a positive control as its effects on bone formation have been described before. Nevertheless, as BMPs demonstrate negative side effects, alternatives, for example, BSP, are urgently required.

We used three groups (empty defect, collagen gel alone [CG], and collagen gel + BMP-7 [CG + BMP-7]) as controls and two test groups (CG + 0.5 μg BSP and CG + 5 μg BSP) with two BSP concentrations. **Figure 2** demonstrates that the created defect represents a critical size defect as even after 8 weeks. No bone regeneration was observed in the group without any implanted material. In the BMP-7 group, the defect is already closed after 3 weeks and the bone thickness increases after 8 weeks. In the CG group, a slight bone formation could be observed after 3 weeks, which has further grown after 8 weeks; a small positive effect of collagen type I alone on bone regeneration has already been described by others[46]. The group with immobilized 0.5 μg BSP showed a similar bone growth like the CG-group, whereas the higher BSP concentration showed an increased bone formation with an almost closed defect after 8 weeks (**Figure 3A and B**).

To further analyze these results, the ratio of BV/TV was calculated using ImageJ. As expected, all groups demonstrated significantly enhanced BV/TV ratios compared to the empty defect group. From the collagen groups, only the positive control with immobilized BMP-7 showed significant differences compared to the CG group. BSP at both concentrations showed no significant differences compared to CG alone although a positive tendency could be observed in the CG group with the higher BSP concentration (**Figure 3C**).

To confirm the results, HE and Masson-Goldner trichrome histological stainings were performed. In the empty defect (**Figure 4**), the two holes are clearly visible, only filled with connective tissue (light rose) and residual bone in the middle (dark pink). Staining of the other groups confirmed the radiological and quantitative results with the highest bone formation seen in the area of the set

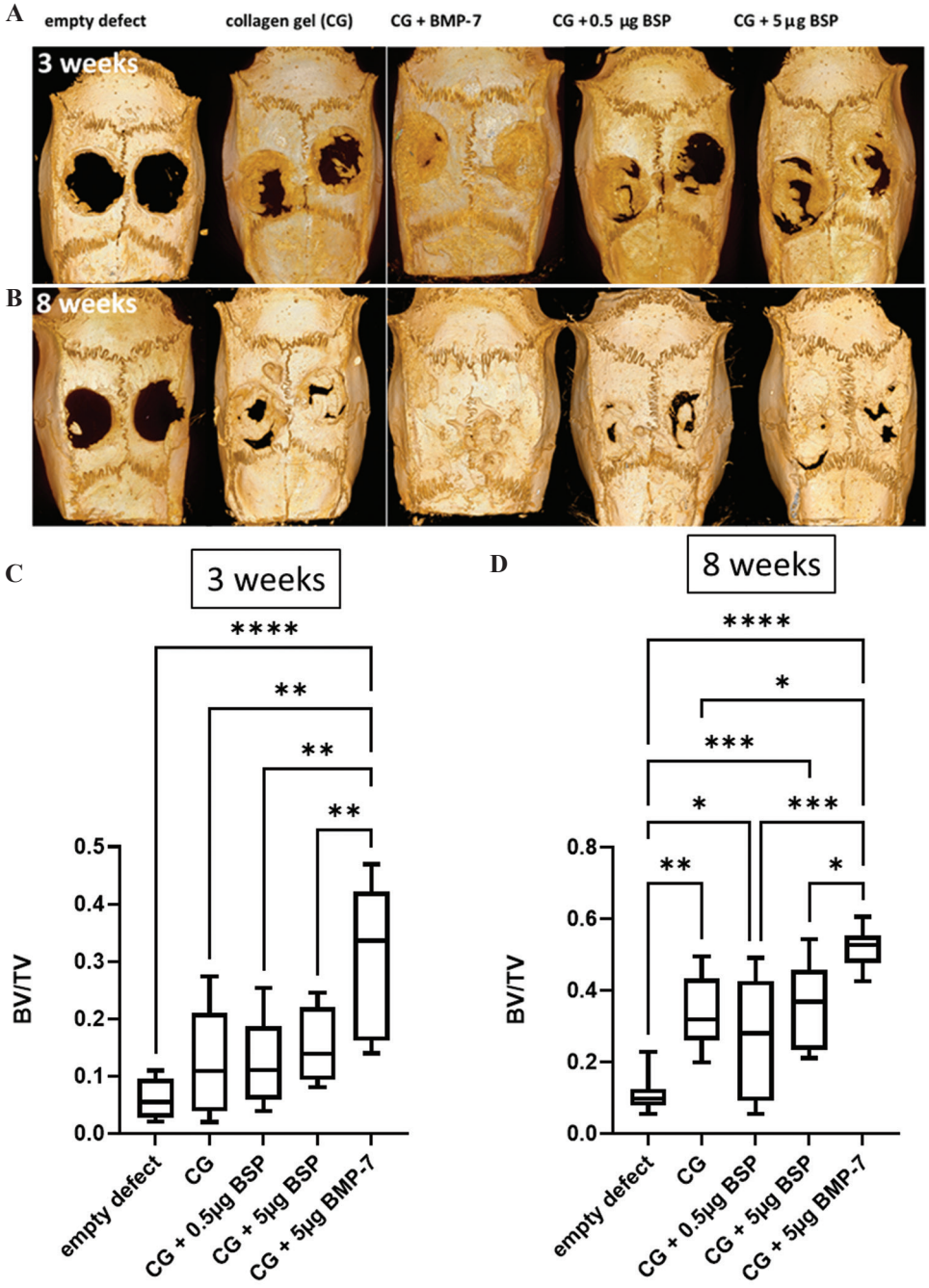

Figure 3. µCt images 3 weeks (A) and 8 weeks (B) after surgery. (C and D) Quantification of results after 3 and 8 weeks. **P* < 0.05, ***P* < 0.01, ****P* < 0.005; *****P* < 0.001 (*n* = 5).

defects in the CG, BMP-7, and BSP groups (**Figure 3,** arrows). The right column shows the Masson-Goldner trichrome staining, where the turquoise stain stands for mineralized bone and corresponds to the HE staining. Interestingly, in the BMP-7 and especially in the 5 µg BSP group, an intense orange staining can be observed representing osteoid tissue.

Comparing our results using collagen with other in vivo models employing implant materials coated with BSP, we observe a better bone regeneration. In a calvarial defect model with calcium phosphate scaffolds coated with BSP, no statistical significances were observed between the groups regarding bone thickness and bone fraction[14]. No positive effect on bone regeneration was observed with the same scaffolds used in a femoral condyle defect model coated with BSP[15]. Considering our results in relation to the literature lead to the hypothesis that the material used as a scaffold plays an important role for the

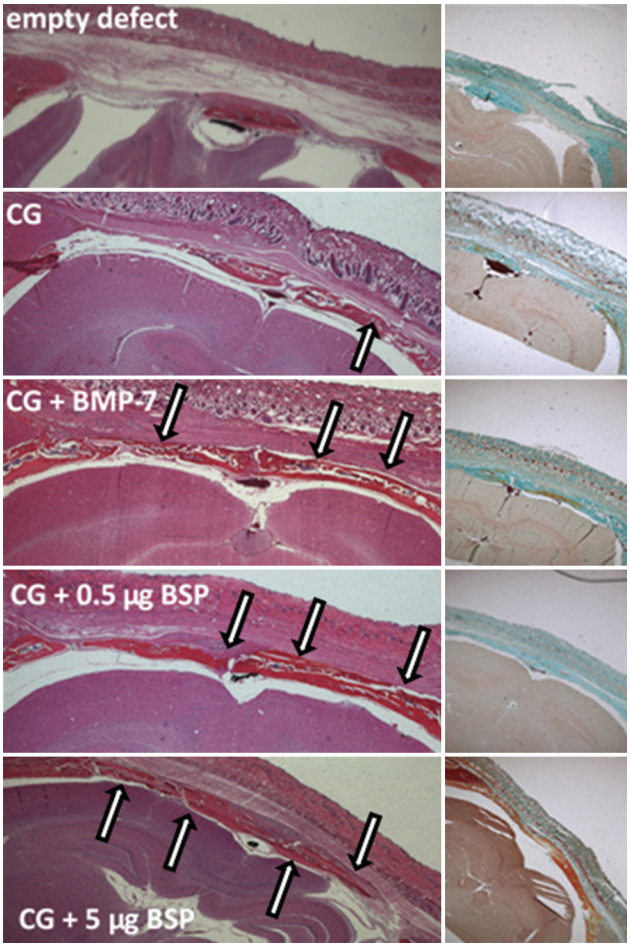

Figure 4. HE and Masson-Goldner trichrome staining 8 weeks after surgery. Arrows indicate newly formed bone.

efficiency of BSP. Gomes *et al*. showed that BSP bound to silk proteins also induces cell viability, and tricalcium phosphate nucleation in osteoblasts in vitro[13]. This confirms our theory that the carrier is important for BSP effects. Regarding collagen gels and polymer scaffolds, it can also be postulated that the surface composition plays an important role for adhesion and growth of osteoblasts. As collagen represents the natural matrix and BSP contains specific binding sites for collagen supporting interaction between these molecules, we hypothesized that collagen type I as an ECM protein is an optimal carrier for BSP and helps to induce the positive effects of BSP.

3.5. Femoral defect model

Although collagen type I has been used in medical applications as carrier material for a long time, one critical aspect particularly concerning bone tissue engineering is its low mechanical stability[47]. To circumvent this problem, we established a combination of polylactide and collagen type I to take advantage of the positive properties of both materials: PLA as mechanically stable material and collagen type I as biodegradable polymer material, which can easily be modified[26,27]. In vitro analyses of this material were performed and demonstrated a good biocompatibility[27]. As described in the method section, we printed a 3D cylinder of polylactide which was filled manually with collagen type I and two different concentrations of BSP. Binding between BSP and collagen type I is provided by the collagen type I binding site of BSP, which has been described in several studies[18,19,22].

BSP release was measured as described in materials and methods and is shown in **Figure S3**. We observed a steady release of BSP over a time period of 72 h. After this time, approximately 60% of the immobilized protein was released, which complies with former studies[26,27]. The dose of 100 ng/ml has been used in various studies. Furthermore, the slow release has been described and is likely to be beneficial for osteogenic regeneration[48]. Our hypothesis is that the missing 40% still remain in the gel and are released in a slow manner, however, further studies with longer time points and determination of the residue dosage have to be performed to confirm this theory.

PLA cylinders were modified with collagen, BSP, or BMP-7 and implanted into a femoral defect of rats. X-rays performed every 2nd week demonstrated the course of bone healing. **Figure 5A** (exemplary images) shows that in the groups with growth factors, either BSP in two concentrations or with BMP-7, the bone defect is almost closed 8 weeks after surgery. Concerning the course of bone growth, it can be observed that BMP-7 shows an earlier begin of bone regeneration than BSP, particularly a directed growth through the cylinder can already be observed 4 weeks after surgery. This effect is even better demonstrated in µCt images processed with the software Osirix (**Figure 5B**).

Figures 5C shows the quantitative analyses of the BV/TV ratio. After 4 weeks, significant differences regarding bone regeneration can be observed in the group with BMP-7 compared to all other groups except to the group with the high BSP concentration. This fact speaks for a fast induction of bone growth in the BMP-7 group, which has already been described in other studies in vitro as well as in vivo[26,49]. After 8 weeks, the bone volume in all groups increased. Especially bone formation in both BSP groups increased significantly compared to the groups without BSP. The BMP-7 group showed the highest BV/TV ratio with significant differences to the groups without growth factors, but the differences compared to the BSP groups were not significant.

Figure 6 displays HE and Masson-Goldner staining of the groups PLA-coll, PLA-coll-BSP high and PLA-coll-BMP-7 as well as the quantitative analyses. Both histological staining confirm the results obtained by X-ray, µCt, and quantitative analyses. In the group without

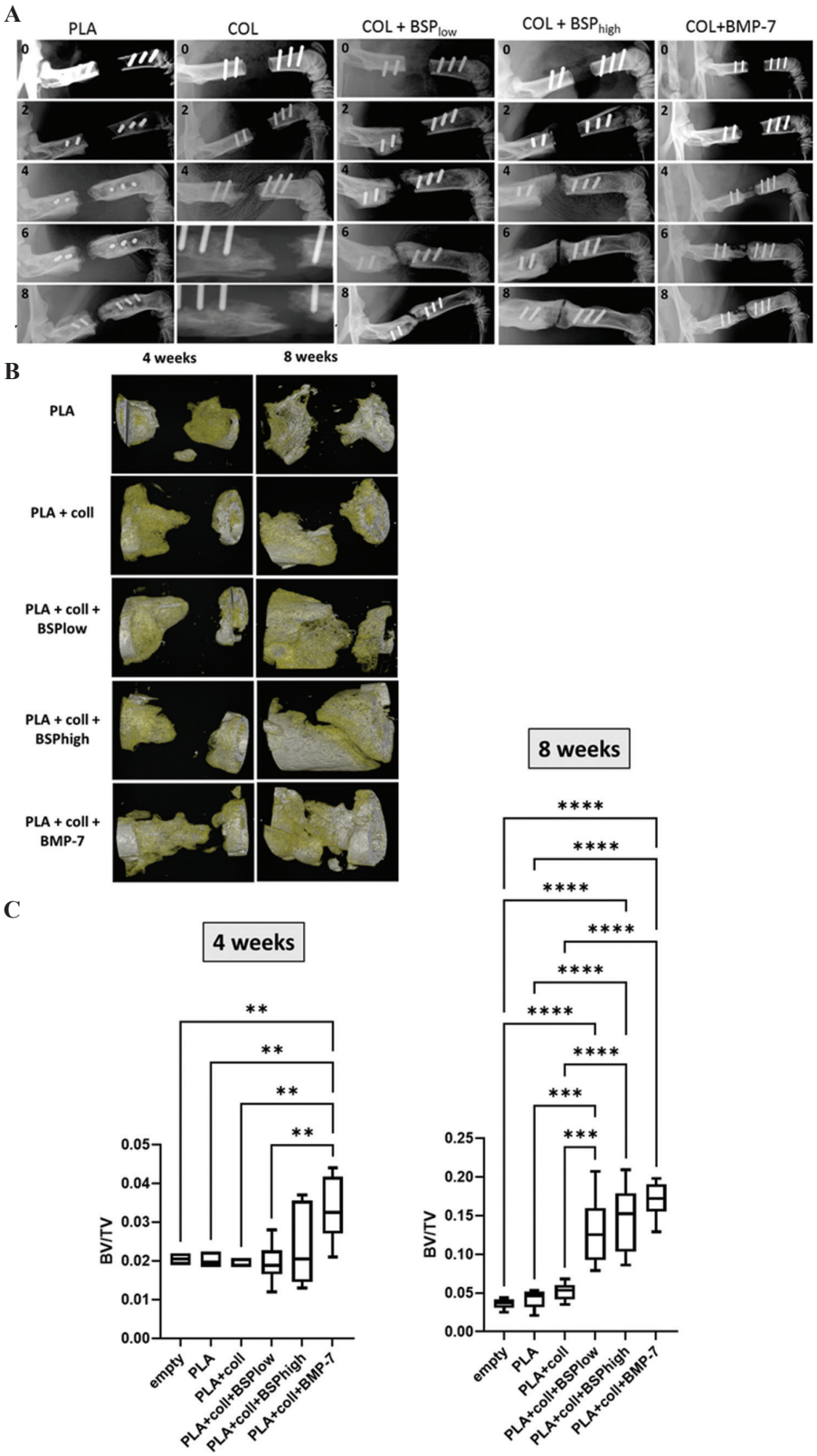

Figure 5. (A) X-ray images every 2 weeks after surgery of the different groups. (B) µCt images processed with Osirix 4 and 8 weeks after surgery and quantitative analyses (BV/TV) 4 and 8 weeks after surgery. (C) After 4 weeks, the BV/TV ratio was highest when PLA cylinders were modified with BMP-7 (**$P < 0.01$). After 8 weeks, the BV/TV ratio was peaking for PLA cylinders modified with BSP or BMP-7 in comparison to empty defects, empty PLA cylinders, and PLA cylinders modified with collagen only (***$P < 0.005$; ****$P < 0.001$).

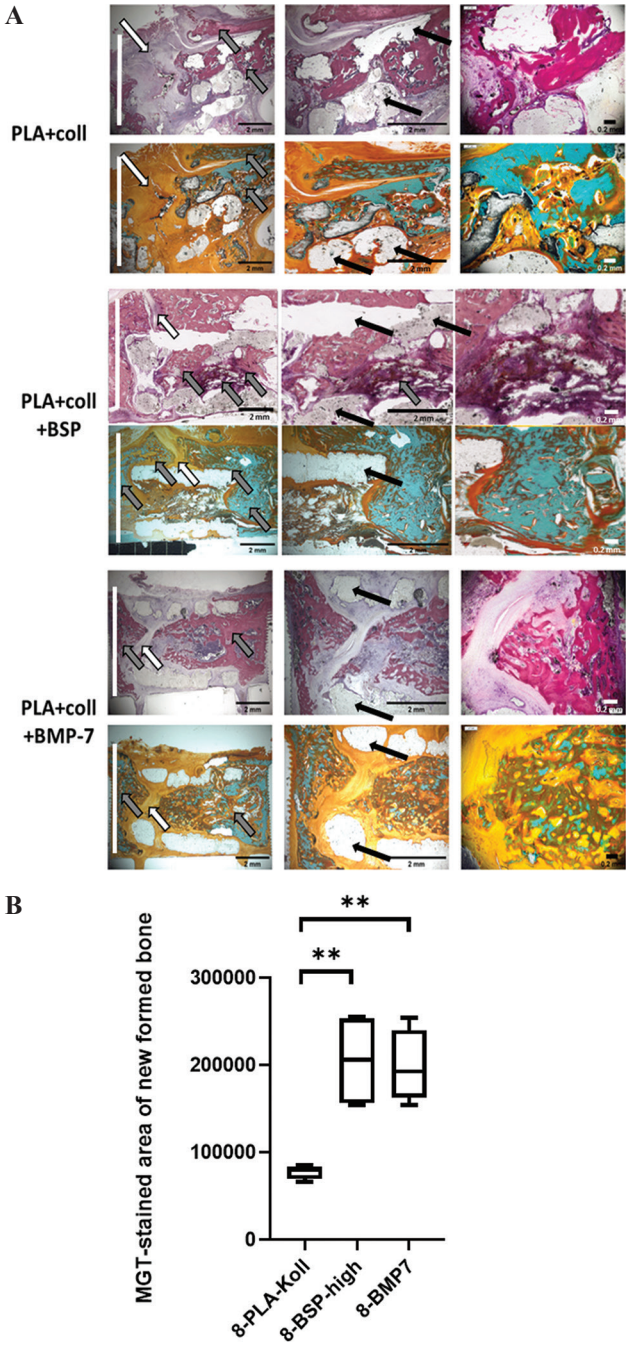

Figure 6. HE and Masson-Goldner trichrome staining 8 weeks after surgery. (A) Areas of collagen and connective tissue show in light pink and beige areas (white arrows), whereas areas with defined bone are dark pink and green/turquoise (gray arrows). The defect edges are marked with a white line and remnants from the PLA cylinder (light areas) are indicated by black arrows. (B) Quantification of results after 8 weeks. $^{**}P < 0.01$; $n = 5$.

growth factors, large areas of collagen and connective tissue were observed (light pink and beige areas; white arrows), whereas only small areas with defined bone were visible (dark pink and green/turquoise areas; gray arrows). The areas representing newly formed bone growing along and inside the PLA cylinder increase in the groups with both growth factors. In the group with BSP, most bone areas are detected around the cylinder and only marginally growing into the cylinder, in the group with BMP-7 growth inside the cylinder was detected and only marginal growth outside the cylinder. These observations are confirmed by quantitative analyses where significant differences are determined regarding area of new formed bone between the control group with collagen alone and the groups with high BSP and BMP7. Interestingly, no significant differences are observed between the groups BSP and BMP-7.

BMP-7 has been used as control as its effects on bone formation have been described in detail[50]. However, administration of BMPs (either BMP-2 or BMP-7) can result in many side effects such as excessive bone formation[51], heterotopic ossification[52], bone with atypical structure or low mechanical stability[53], inflammatory complications or massive soft-tissue swelling, or tumor formation[54].

By reflecting former results regarding BSP immobilized on titanium or CPC[11,12,14,15] and comparing them with the results of the presented study, we confirmed our hypothesis that the best effects of BSP are achieved when BSP is coupled to collagen type I. It is known that BSP contains a collagen-binding site[19] and several effects regarding the interaction between collagen and BSP have been described. Choi *et al*. showed that the collagen interaction promoted hydroxyapatite nucleation and that a collagen-binding peptide derived from BSP increased osteogenic differentiation in muscle-derived stem cells and induced expression of osteoblastic marker genes and proteins without affecting proliferation[55]. Last but not least, Choi *et al*. showed coating of hydroxyapatite scaffolds with the collagen-binding peptide-induced bone formation in a craniotomy defect in rabbits[56]. Similar effects were observed in a rat calvarial model[20,21], where they found induced calcification. Comparing their studies with ours, they used higher concentrations than we did (20 μg/implant). Moreover, they did not show any data on bone regeneration by X-rays or μCt analyses, but only histological pictures after 30 days, which makes an interpretation and comparison to our results difficult. In our study, two different BSP concentrations were used, both resulting in statistically significant differences in bone growth when compared to the groups without BSP. Moreover, compared to the positive control with BMP-7, no statistically significant differences were observed after 8 weeks, speaking for a very positive effect of BSP on bone regeneration when combined with collagen type I.

The interactions between BSP and collagen have been reviewed by Kruger *et al*., 2013,[22] and other studies describing various effects of BSP in combination with collagen. Chou *et al*. described a positive effect of BSP

on the interconnection of tendon and bone[57] and Wang found that BSP collagen in subcutaneous pouches did not induce calcification. These results are confirmed by our data.

Most in vivo studies describing a positive effect of BSP in regard to bone regeneration were performed in a cranial model, where no mechanical stability of the implant is needed. In our femora model, we combined PLA with collagen type I and BSP to receive a mechanically stable osteoinductive implant, whose mechanical stability has been demonstrated in a former study[26]. The combination of collagen type I with 3D-printed polylactide structures has been used before. However, most studies describe osteogenic effects when 3D-printed PLA scaffolds were surface coated with collagen type I and/or other bioactive molecules[58,59] and not when bioactive molecules were incorporated into a polylactide scaffold. Our study is the first to demonstrate the positive effect of BSP when incorporated into collagen type I.

4. Conclusion

In our study, we could show that BSP incorporated into collagen type I enhances osteogenic effects in vitro as well as in vivo. Especially the combination with 3D-printed polylactide demonstrated positive results regarding bridging of a critical size bone defect in a femora rat model. This 3D-biofabricated cell-free biomaterial consisting of PLA and collagen type I with incorporated BSP can be easily produced and is a promising biomaterial to be further analyzed for its application as bone substitute material.

Acknowledgments

This work is part of the doctoral theses of Anja Kriegel, Christian Schlosser, and Christoph Dahmen. We thank the tissue bank of the University Medical Center Mainz for their support in histological analyses.

Funding

This project was funded by Immundiagnostik AG.

Conflicts of interest

Franz Paul Armbruster is the CEO of Immundiagnostik AG and Franziska Clauder is the employee of Immundiagnostik AG. All other authors state no conflicts of interest.

Authors' contributions

Conceptualization: Ulrike Ritz, Philipp Drees, Pol Maria Rommens, and Franz Paul Armbruster

Data curation: Andreas Baranowski, Ulrike Ritz, and Anja Kriegel

Formal analysis: Anja Kriegel, Ulrike Ritz, and Hermann Götz

Funding acquisition: Franz Paul Armbruster

Investigation: Anja Kriegel, Christian Schlosser, Tanja Habeck, and Christoph Dahmen

Methodology: Anja Kriegel, Andreas Baranowski, Hermann Götz, and Ulrike Ritz

Project administration: Ulrike Ritz

Resources: Philipp Drees, Franz Paul Armbruster, and Pol Maria Rommens

Validation: Anja Kriegel, Ulrike Ritz, and Andreas Baranowski

Writing – original draft: Ulrike Ritz

Writing – review and editing: Anja Kriegel, Ulrike Ritz, Andreas Baranowski, Franziska Clauder, Philipp Drees, and Pol Maria Rommens.

Availability of data

The raw/processed data required to reproduce these findings cannot be shared at this time due to technical or time limitations.

References

1. Florencio-Silva R, Sasso GR, Sasso-Cerri E, *et al.*, 2015, Biology of Bone Tissue: Structure, Function, and Factors That Influence Bone Cells. *Biomed Res Int*, 2015:421746. https://doi.org/1155/2015/421746
2. Staines KA, MacRae VE, Farquharson C, 2012, The Importance of the SIBLING Family of Proteins on Skeletal Mineralisation and Bone Remodelling. *J Endocrinol*, 214:241–55. https://doi.org/1530/JOE-12-0143
3. Vincent K, Durrant MC, 2013, A Structural and Functional Model for Human Bone Sialoprotein. *J Mol Graph Model*, 39:108–17. https://doi.org/1016/j.jmgm.2012.10.007
4. Gordon JA, Tye CE, Sampaio AV, *et al.*, 2007, Bone Sialoprotein Expression Enhances Osteoblast Differentiation and Matrix Mineralization In Vitro. *Bone*, 41:462–73. https://doi.org/1016/j.bone.2007.04.191
5. Bouleftour W, Juignet L, Bouet G, *et al.*, 2016, The Role of the SIBLING, Bone Sialoprotein in Skeletal Biology Contribution of Mouse Experimental Genetics. *Matrix Biol*, 52–54:60–77. https://doi.org/1016/j.matbio.2015.12.011
6. Monfoulet L, Malaval L, Aubin JE, *et al.*, 2010, Bone Sialoprotein, but not Osteopontin, Deficiency Impairs the Mineralization of Regenerating Bone during Cortical Defect Healing. *Bone*, 46:447–52.

https://doi.org/1016/j.bone.2009.09.007

7. Boudiffa M, Wade-Gueye NM, Guignandon A, *et al.*, 2010, Bone Sialoprotein Deficiency Impairs Osteoclastogenesis and Mineral Resorption In Vitro. *J Bone Miner Res*, 25:2669–79. https://doi.org/1002/jbmr.245
8. Malaval L, Wade-Gueye NM, Boudiffa M, *et al.*, 2008, Bone Sialoprotein Plays a Functional Role in Bone Formation and Osteoclastogenesis. *J Exp Med*, 205:1145–53. https://doi.org/1084/jem.20071294
9. Bouleftour W, Juignet L, Verdiere L, *et al.*, 2019, Deletion of OPN in BSP Knockout Mice does not Correct Bone Hypomineralization but Results in High Bone Turnover. *Bone*, 120:411–22. https://doi.org/1016/j.bone.2018.12.001
10. Holm E, Aubin JE, Hunter GK, *et al.*, 2015, Loss of Bone Sialoprotein Leads to Impaired Endochondral Bone Development and Mineralization. *Bone*, 71:145–54. https://doi.org/1016/j.bone.2014.10.007
11. Baranowski A, Klein A, Ritz U, *et al.*, 2016, Surface Functionalization of Orthopedic Titanium Implants with Bone Sialoprotein. *PLoS One*, 11:e0153978. https://doi.org/1371/journal.pone.0153978
12. Klein A, Baranowski A, Ritz U, *et al.*, 2018, Effect of Bone Sialoprotein Coated Three-dimensional Printed Calcium Phosphate Scaffolds on Primary Human Osteoblasts. *J Biomed Mater Res B Appl Biomater*, 106:2565–75. https://doi.org/1002/jbm.b.34073
13. Gomes S, Gallego-Llamas J, Leonor IB, *et al.*, 2013, In Vivo Biological Responses to Silk Proteins Functionalized with Bone Sialoprotein. *Macromol Biosci*, 13:444–54. https://doi.org/1002/mabi.201200372
14. Baranowski A, Klein A, Ritz U, *et al.*, 2018, Evaluation of Bone Sialoprotein Coating of Three-Dimensional Printed Calcium Phosphate Scaffolds in a Calvarial Defect Model in Mice. *Materials* (*Basel*), 11:2336. https://doi.org/3390/ma11112336
15. Klein A, Baranowski A, Ritz U, *et al.*, 2020, Effect of Bone Sialoprotein Coating on Progression of Bone Formation in a Femoral Defect Model in Rats. *Eur J Trauma Emerg Surg*, 46:277–86. https://doi.org/1007/s00068-019-01159-5
16. Wallace DG, Rosenblatt J, 2003, Collagen Gel Systems for Sustained Delivery and Tissue Engineering. *Adv Drug Deliv Rev*, 55:1631–49.
17. Bierbaum S, Hintze V, Scharnweber D, 2012, Functionalization of Biomaterial Surfaces Using Artificial Extracellular Matrices. *Biomatter*, 2:132–41. https://doi.org/4161/biom.20921
18. Motamedian SR, Hosseinpour S, Ahsaie MG, *et al.*, 2015, Smart Scaffolds in Bone Tissue Engineering: A Systematic Review of Literature. *World J Stem Cells*, 7:657–68. https://doi.org/4252/wjsc.v7.i3.657
19. Tye CE, Hunter GK, Goldberg HA, 2005, Identification of the Type I Collagen-binding Domain of Bone Sialoprotein and Characterization of the Mechanism of Interaction. *J Biol Chem*., 280:13487–92. https://doi.org/1074/jbc.M408923200
20. Wang J, Zhou HY, Salih E, *et al.*, 2006, Site-specific In Vivo Calcification and Osteogenesis Stimulated by Bone Sialoprotein. *Calcif Tissue Int*, 79:179–89. https://doi.org/1007/s00223-006-0018-2
21. Xu L, Anderson AL, Lu Q, *et al.*, 2007, Role of Fibrillar Structure of Collagenous Carrier in Bone Sialoprotein-mediated Matrix Mineralization and Osteoblast Differentiation. *Biomaterials*, 28:750–61. https://doi.org/1016/j.biomaterials.2006.09.022
22. Kruger TE, Miller AH, Wang J, 2013, Collagen Scaffolds in Bone Sialoprotein-Mediated Bone Regeneration. *ScientificWorldJournal*, 2013:812718. https://doi.org/1155/2013/812718
23. Gorski JP, Franz NT, Pernoud D, *et al.*, 2021, A Repeated Triple Lysine Motif Anchors Complexes Containing Bone Sialoprotein and the type XI Collagen A1 Chain Involved in Bone Mineralization. *J Biol Chem*, 296:100436. https://doi.org/1016/j.jbc.2021.100436
24. Serra T, Mateos-Timoneda MA, Planell JA, *et al.*, 2013, 3D Printed PLA-based Scaffolds: A Versatile Tool in Regenerative Medicine. *Organogenesis*, 9:239–44. https://doi.org/4161/org.26048
25. Guvendiren M, Molde J, Soares RM, *et al.*, 2016, Designing Biomaterials for 3D Printing. *ACS Biomater Sci Eng*, 2:1679–93. https://doi.org/1021/acsbiomaterials.6b00121
26. Lauer A, Wolf P, Mehler D, *et al.*, 2020, Biofabrication of SDF-1 Functionalized 3D-Printed Cell-Free Scaffolds for Bone Tissue Regeneration. *Int J Mol Sci*, 21:2175. https://doi.org/3390/ijms21062175
27. Ritz U, Gerke R, Gotz H, *et al.*, 2017, A New Bone Substitute Developed from 3D-Prints of Polylactide (PLA) Loaded with Collagen I: An In Vitro Study. *Int J Mol Sci*, 18:2569. https://doi.org/3390/ijms18122569
28. Martin V, Ribeiro IA, Alves MM, *et al.*, 2019, Engineering a Multifunctional 3D-Printed PLA-collagen-minocycline-nanoHydroxyapatite Scaffold with Combined Antimicrobial and Osteogenic Effects for Bone Regeneration. *Mater Sci*

Eng C Mater Biol Appl, 101:15–26.
https://doi.org/1016/j.msec.2019.03.056

29. Dewey MJ, Johnson EM, Weisgerber DW, *et al.*, 2019, Shape-fitting Collagen-PLA Composite Promotes Osteogenic Differentiation of Porcine Adipose Stem Cells. *J Mech Behav Biomed Mater*, 95:21–33.
https://doi.org/1016/j.jmbbm.2019.03.017
30. Hofmann A, Ritz U, Verrier S, *et al.*, 2008, The Effect of Human Osteoblasts on Proliferation and Neo-vessel Formation of Human Umbilical Vein Endothelial Cells in a Long-term 3D Co-culture on Polyurethane Scaffolds. *Biomaterials*, 29:4217–26.
https://doi.org/1016/j.biomaterials.2008.07.024
31. Wenger A, Stahl A, Weber H, *et al.*, 2004, Modulation of In Vitro Angiogenesis in a Three-dimensional Spheroidal Coculture Model for Bone Tissue Engineering. *Tissue Eng*, 10:1536–47.
https://doi.org/1089/ten.2004.10.1536
32. Livak KJ, Schmittgen TD, 2001, Analysis of Relative Gene Expression Data Using Real-time Quantitative PCR and the 2(-Delta Delta C(T)) Method. *Methods*, 25:402–8.
https://doi.org/1006/meth.2001.1262
33. Schindelin J, Rueden CT, Hiner MC, *et al.*, 2015, The ImageJ Ecosystem: An Open Platform for Biomedical Image Analysis. *Mol Reprod Dev*, 82:518–29.
https://doi.org/1002/mrd.22489
34. Doube M, Klosowski MM, Arganda-Carreras I, *et al.*, 2010, BoneJ: Free and Extensible Bone Image Analysis in ImageJ. *Bone*, 47:1076–9.
https://doi.org/1016/j.bone.2010.08.023
35. Unger RE, Dohle E, Kirkpatrick CJ, 2015, Improving Vascularization of Engineered Bone through the Generation of Pro-angiogenic Effects in Co-culture Systems. *Adv Drug Deliv Rev*, 94:116–25.
https://doi.org/1016/j.addr.2015.03.012
36. Unger RE, Halstenberg S, Sartoris A, *et al.*, 2011, Human Endothelial and Osteoblast Co-cultures on 3D Biomaterials. *Methods Mol Biol*, 695:229–41.
https://doi.org/1007/978-1-60761-984-0_15
37. Xia B, Wang J, Guo L, *et al.*, 2011, Effect of Bone Sialoprotein on Proliferation and Osteodifferentiation of Human Bone Marrow-derived Mesenchymal Stem Cells In Vitro. *Biologicals*, 39:217–23.
https://doi.org/1016/j.biologicals.2011.04.004
38. Shi Z, Neoh KG, Kang ET, *et al.*, 2009, Surface Functionalization of Titanium with Carboxymethyl Chitosan and Immobilized Bone Morphogenetic Protein-2 for Enhanced Osseointegration. *Biomacromolecules*, 10:1603–11.
https://doi.org/1021/bm900203w
39. van der Zande M, Walboomers XF, Briest A, *et al.*, 2008, The Effect of Combined Application of TGFbeta-1, BMP-2, and COLLOSS E on the Development of Bone Marrow Derived Osteoblast-like Cells In Vitro. *J Biomed Mater Res Part A*, 86:788–95.
https://doi.org/1002/jbm.a.31645
40. Deckers MM, van Bezooijen RL, van der Horst G, *et al.*, 2002, Bone Morphogenetic Proteins Stimulate Angiogenesis through Osteoblast-derived Vascular Endothelial Growth Factor A. *Endocrinology*, 143:1545–53.
https://doi.org/1210/endo.143.4.8719
41. Im B J, Lee SC, Lee MH, *et al.*, 2016, Promotion of Osteoblastic Differentiation and Osteogenic Transcription Factor Expression on a Microgroove Titanium Surface with Immobilized Fibronectin or Bone Sialoprotein II. *Biomed Mater*, 11:035020.
https://doi.org/1088/1748-6041/11/3/035020
42. Schaeren S, Jaquiery C, Wolf F, *et al.*, 2010, Effect of Bone Sialoprotein Coating of Ceramic and Synthetic Polymer Materials on In Vitro Osteogenic Cell Differentiation And *In Vivo* Bone Formation. *J Biomed Mater Res Part A*, 92:1461–7.
https://doi.org/1002/jbm.a.32459
43. Fujisawa R, Nodasaka Y, Kuboki Y, 1995, Further Characterization of Interaction Between Bone Sialoprotein (BSP) and Collagen. *Calcif Tissue Int*, 56:140–4.
https://doi.org/1007/BF00296346
44. Baht GS, Hunter GK, Goldberg HA, 2008, Bone Sialoprotein-collagen Interaction Promotes Hydroxyapatite Nucleation. *Matrix Biol*, 27:600–8.
https://doi.org/1016/j.matbio.2008.06.004
45. Hudieb M, Haddad A, Bakeer M, *et al.*, 2021, Influence of Age on Calvarial Critical Size Defect Dimensions: A Radiographic and Histological Study. *J Craniofac Surg*, 32:2896–900.
https://doi.org/1097/SCS.0000000000007690
46. Forster Y, Rentsch C, Schneiders W, *et al.*, 2012, Surface Modification of Implants in Long Bone. *Biomatter*, 2:149–57.
https://doi.org/4161/biom.21563
47. Bielajew BJ, Hu JC, Athanasiou KA, 2020, Collagen: Quantification, Biomechanics and Role of Minor Subtypes in Cartilage. *Nat Rev Mater*, 5:730–47.
https://doi.org/1038/s41578-020-0213-1
48. Zang S, Mu R, Chen F, *et al.*, 2019, Injectable Chitosan/Beta-glycerophosphate Hydrogels with Sustained Release of BMP-7 and Ornidazole in Periodontal Wound Healing

of Class III Furcation Defects. *Mater Sci Eng C Mater Biol Appl*, 99:919–28.
https://doi.org/1016/j.msec.2019.02.024

49. Schlickewei C, Klatte TO, Wildermuth Y, *et al.*, 2019, A Bioactive Nano-calcium Phosphate Paste for *In-Situ* Transfection of BMP-7 and VEGF-A in a Rabbit Critical-size Bone Defect: Results of an In Vivo Study. *J Mater Sci Mater Med*, 30:15.
https://doi.org/1007/s10856-019-6217-y
50. El Bialy I, Jiskoot W, Nejadnik MR, 2017, Formulation, Delivery and Stability of Bone Morphogenetic Proteins for Effective Bone Regeneration. *Pharm Res*, 34:1152–70.
https://doi.org/1007/s11095-017-2147-x
51. Ritz U, Eberhardt M, Klein A, *et al.*, 2018, Photocrosslinked Dextran-Based Hydrogels as Carrier System for the Cells and Cytokines Induce Bone Regeneration in Critical Size Defects in Mice. *Gels*, 4:63.
https://doi.org/3390/gels4030063
52. Papanagiotou M, Dailiana ZH, Karachalios T, *et al.*, 2017, Heterotopic Ossification after the Use of Recombinant Human Bone Morphogenetic Protein-7. *World J Orthop*, 8:36–41.
https://doi.org/5312/wjo.v8.i1.36
53. Williams JC, Maitra S, Anderson MJ, *et al.*, 2015, BMP-7 and Bone Regeneration: Evaluation of Dose-Response in a Rodent Segmental Defect Model. *J Orthop Trauma*, 29:e336–41.
https://doi.org/1097/BOT.0000000000000307
54. Gillman CE, Jayasuriya AC, 2021, FDA-approved Bone Grafts and Bone Graft Substitute Devices in Bone Regeneration. *Mater Sci Eng C Mater Biol Appl*, 130:112466.
https://doi.org/1016/j.msec.2021.112466
55. Choi YJ, Lee JY, Lee SJ, *et al.*, 2012, Determination of Osteogenic or Adipogenic Lineages in Muscle-derived Stem Cells (MDSCs) by a Collagen-binding Peptide (CBP) Derived from Bone Sialoprotein (BSP). *Biochem Biophys Res Commun*, 419:326–32.
https://doi.org/1016/j.bbrc.2012.02.022
56. Choi YJ, Lee JY, Chung CP, *et al.*, 2013, Enhanced Osteogenesis by Collagen-binding Peptide from Bone Sialoprotein In Vitro and In Vivo. *J Biomed Mater Res Part A*, 101:547–54.
https://doi.org/1002/jbm.a.34356
57. Chou YC, Yeh WL, Chao CL, *et al.*, 2016, Enhancement of Tendon-bone Healing via the Combination of Biodegradable Collagen-loaded Nanofibrous Membranes and a Three-dimensional Printed Bone-anchoring Bolt. *Int J Nanomed*, 11:4173–86.
https://doi.org/2147/IJN.S108939
58. Nashchekina Y, Nikonov P, Nashchekin A, *et al.*, 2020, Functional Polylactide Blend Films for Controlling Mesenchymal Stem Cell Behaviour. *Polymers* (*Basel*), 12:1969.
https://doi.org/3390/polym12091969
59. Teixeira BN, Aprile P, Mendonca RH, *et al.*, 2019, Evaluation of Bone Marrow Stem Cell Response to PLA Scaffolds Manufactured by 3D Printing and Coated with Polydopamine and Type I Collagen. *J Biomed Mater Res B Appl Biomater*, 107:37–49.
https://doi.org/1002/jbm.b.34093

Publisher's note